Search for charged Higgs bosons in top quark decays

V.M. Abazov[37], B. Abbott[75], M. Abolins[65], B.S. Acharya[30], M. Adams[51], T. Adams[49], E. Aguilo[6], M. Ahsan[59], G.D. Alexeev[37], G. Alkhazov[41], A. Alton[64,a], G. Alverson[63], G.A. Alves[2], L.S. Ancu[36], M.S. Anzelc[53], M. Aoki[50], Y. Arnoud[14], M. Arov[60], M. Arthaud[18], A. Askew[49,b], B. Åsman[42], O. Atramentov[49,b], C. Avila[8], J. BackusMayes[82], F. Badaud[13], L. Bagby[50], B. Baldin[50], D.V. Bandurin[59], S. Banerjee[30], E. Barberis[63], A.-F. Barfuss[15], P. Bargassa[80], P. Baringer[58], J. Barreto[2], J.F. Bartlett[50], U. Bassler[18], D. Bauer[44], S. Beale[6], A. Bean[58], M. Begalli[3], M. Begel[73], C. Belanger-Champagne[42], L. Bellantoni[50], A. Bellavance[50], J.A. Benitez[65], S.B. Beri[28], G. Bernardi[17], R. Bernhard[23], I. Bertram[43], M. Besançon[18], R. Beuselinck[44], V.A. Bezzubov[40], P.C. Bhat[50], V. Bhatnagar[28], G. Blazey[52], S. Blessing[49], K. Bloom[67], A. Boehnlein[50], D. Boline[62], T.A. Bolton[59], E.E. Boos[39], G. Borissov[43], T. Bose[62], A. Brandt[78], R. Brock[65], G. Brooijmans[70], A. Bross[50], D. Brown[19], X.B. Bu[7], D. Buchholz[53], M. Buehler[81], V. Buescher[22], V. Bunichev[39], S. Burdin[43,c], T.H. Burnett[82], C.P. Buszello[44], P. Calfayan[26], B. Calpas[15], S. Calvet[16], J. Cammin[71], M.A. Carrasco-Lizarraga[34], E. Carrera[49], W. Carvalho[3], B.C.K. Casey[50], H. Castilla-Valdez[34], S. Chakrabarti[72], D. Chakraborty[52], K.M. Chan[55], A. Chandra[48], E. Cheu[46], D.K. Cho[62], S.W. Cho[32], S. Choi[33], B. Choudhary[29], T. Christoudias[44], S. Cihangir[50], D. Claes[67], J. Clutter[58], M. Cooke[50], W.E. Cooper[50], M. Corcoran[80], F. Couderc[18], M.-C. Cousinou[15], D. Cutts[77], M. Ćwiok[31], A. Das[46], G. Davies[44], K. De[78], S.J. de Jong[36], E. De La Cruz-Burelo[34], K. DeVaughan[67], F. Déliot[18], M. Demarteau[50], R. Demina[71], D. Denisov[50], S.P. Denisov[40], S. Desai[50], H.T. Diehl[50], M. Diesburg[50], A. Dominguez[67], T. Dorland[82], A. Dubey[29], L.V. Dudko[39], L. Duflot[16], D. Duggan[49], A. Duperrin[15], S. Dutt[28], A. Dyshkant[52], M. Eads[67], D. Edmunds[65], J. Ellison[48], V.D. Elvira[50], Y. Enari[77], S. Eno[61], M. Escalier[15], H. Evans[54], A. Evdokimov[73], V.N. Evdokimov[40], G. Facini[63], A.V. Ferapontov[59], T. Ferbel[61,71], F. Fiedler[25], F. Filthaut[36], W. Fisher[50], H.E. Fisk[50], M. Fortner[52], H. Fox[43], S. Fu[50], S. Fuess[50], T. Gadfort[70], C.F. Galea[36], A. Garcia-Bellido[71], V. Gavrilov[38], P. Gay[13], W. Geist[19], W. Geng[15,65], C.E. Gerber[51], Y. Gershtein[49,b], D. Gillberg[6], G. Ginther[50,71], B. Gómez[8], A. Goussiou[82], P.D. Grannis[72], S. Greder[19], H. Greenlee[50], Z.D. Greenwood[60], E.M. Gregores[4], G. Grenier[20], Ph. Gris[13], J.-F. Grivaz[16], A. Grohsjean[18], S. Grünendahl[50], M.W. Grünewald[31], F. Guo[72], J. Guo[72], G. Gutierrez[50], P. Gutierrez[75], A. Haas[70], P. Haefner[26], S. Hagopian[49], J. Haley[68], I. Hall[65], R.E. Hall[47], L. Han[7], K. Harder[45], A. Harel[71], J.M. Hauptman[57], J. Hays[44], T. Hebbeker[21], D. Hedin[52], J.G. Hegeman[35], A.P. Heinson[48], U. Heintz[62], C. Hensel[24], I. Heredia-De La Cruz[34], K. Herner[64], G. Hesketh[63], M.D. Hildreth[55], R. Hirosky[81], T. Hoang[49], J.D. Hobbs[72], B. Hoeneisen[12], M. Hohlfeld[22], S. Hossain[75], P. Houben[35], Y. Hu[72], Z. Hubacek[10], N. Huske[17], V. Hynek[10], I. Iashvili[69], R. Illingworth[50], A.S. Ito[50], S. Jabeen[62], M. Jaffré[16], S. Jain[75], K. Jakobs[23], D. Jamin[15], R. Jesik[44], K. Johns[46], C. Johnson[70], M. Johnson[50], D. Johnston[67], A. Jonckheere[50], P. Jonsson[44], A. Juste[50], E. Kajfasz[15], D. Karmanov[39], P.A. Kasper[50], I. Katsanos[67], V. Kaushik[78], R. Kehoe[79], S. Kermiche[15], N. Khalatyan[50], A. Khanov[76], A. Kharchilava[69], Y.N. Kharzheev[37], D. Khatidze[77], M.H. Kirby[53], M. Kirsch[21], B. Klima[50], J.M. Kohli[28], J.-P. Konrath[23], A.V. Kozelov[40], J. Kraus[65], T. Kuhl[25], A. Kumar[69], A. Kupco[11], T. Kurča[20], V.A. Kuzmin[39], J. Kvita[9], F. Lacroix[13], D. Lam[55], S. Lammers[54], G. Landsberg[77], P. Lebrun[20], H.S. Lee[32], W.M. Lee[50], A. Leflat[39], J. Lellouch[17], L. Li[48], Q.Z. Li[50], S.M. Lietti[5], J.K. Lim[32], D. Lincoln[50], J. Linnemann[65], V.V. Lipaev[40], R. Lipton[50], Y. Liu[7], Z. Liu[6], A. Lobodenko[41], M. Lokajicek[11], P. Love[43], H.J. Lubatti[82], R. Luna-Garcia[34,d], A.L. Lyon[50], A.K.A. Maciel[2], D. Mackin[80], P. Mättig[27], R. Magaña-Villalba[34], P.K. Mal[46], S. Malik[67], V.L. Malyshev[37], Y. Maravin[59], B. Martin[14], R. McCarthy[72], C.L. McGivern[58], M.M. Meijer[36], A. Melnitchouk[66], L. Mendoza[8], D. Menezes[52], P.G. Mercadante[5], M. Merkin[39], K.W. Merritt[50], A. Meyer[21], J. Meyer[24], N.K. Mondal[30], R.W. Moore[6], T. Moulik[58], G.S. Muanza[15], M. Mulhearn[70], O. Mundal[22], L. Mundim[3], E. Nagy[15], M. Naimuddin[50], M. Narain[77], H.A. Neal[64], J.P. Negret[8], P. Neustroev[41], H. Nilsen[23], H. Nogima[3], S.F. Novaes[5], T. Nunnemann[26], G. Obrant[41], C. Ochando[16], D. Onoprienko[59], J. Orduna[34], N. Oshima[50], N. Osman[44], J. Osta[55], R. Otec[10], G.J. Otero y Garzón[1], M. Owen[45], M. Padilla[48], P. Padley[80], M. Pangilinan[77], N. Parashar[56], S.-J. Park[24], S.K. Park[32], J. Parsons[70], R. Partridge[77], N. Parua[54], A. Patwa[73], B. Penning[23], M. Perfilov[39], K. Peters[45], Y. Peters[45], P. Pétroff[16], R. Piegaia[1], J. Piper[65], M.-A. Pleier[22], P.L.M. Podesta-Lerma[34,e], V.M. Podstavkov[50], Y. Pogorelov[55], M.-E. Pol[2], P. Polozov[38], A.V. Popov[40], M. Prewitt[80], S. Protopopescu[73], J. Qian[64], A. Quadt[24], B. Quinn[66], A. Rakitine[43], M.S. Rangel[16], K. Ranjan[29], P.N. Ratoff[43], P. Renkel[79], P. Rich[45], M. Rijssenbeek[72], I. Ripp-Baudot[19], F. Rizatdinova[76], S. Robinson[44], M. Rominsky[75], C. Royon[18], P. Rubinov[50], R. Ruchti[55], G. Safronov[38], G. Sajot[14], A. Sánchez-Hernández[34], M.P. Sanders[26], B. Sanghi[50], G. Savage[50], L. Sawyer[60], T. Scanlon[44], D. Schaile[26], R.D. Schamberger[72], Y. Scheglov[41], H. Schellman[53], T. Schliephake[27], S. Schlobohm[82], C. Schwanenberger[45], R. Schwienhorst[65],

J. Sekaric[49], H. Severini[75], E. Shabalina[24], M. Shamim[59], V. Shary[18], A.A. Shchukin[40], R.K. Shivpuri[29], V. Siccardi[19], V. Simak[10], V. Sirotenko[50], P. Skubic[75], P. Slattery[71], D. Smirnov[55], G.R. Snow[67], J. Snow[74], S. Snyder[73], S. Söldner-Rembold[45], L. Sonnenschein[21], A. Sopczak[43], M. Sosebee[78], K. Soustruznik[9], B. Spurlock[78], J. Stark[14], V. Stolin[38], D.A. Stoyanova[40], J. Strandberg[64], M.A. Strang[69], E. Strauss[72], M. Strauss[75], R. Ströhmer[26], D. Strom[51], L. Stutte[50], S. Sumowidagdo[49], P. Svoisky[36], M. Takahashi[45], A. Tanasijczuk[1], W. Taylor[6], B. Tiller[26], M. Titov[18], V.V. Tokmenin[37], I. Torchiani[23], D. Tsybychev[72], B. Tuchming[18], C. Tully[68], P.M. Tuts[70], R. Unalan[65], L. Uvarov[41], S. Uvarov[41], S. Uzunyan[52], P.J. van den Berg[35], R. Van Kooten[54], W.M. van Leeuwen[35], N. Varelas[51], E.W. Varnes[46], I.A. Vasilyev[40], P. Verdier[20], L.S. Vertogradov[37], M. Verzocchi[50], M. Vesterinen[45], D. Vilanova[18], P. Vint[44], P. Vokac[10], R. Wagner[68], H.D. Wahl[49], M.H.L.S. Wang[71], J. Warchol[55], G. Watts[82], M. Wayne[55], G. Weber[25], M. Weber[50,f], L. Welty-Rieger[54], A. Wenger[23,g], M. Wetstein[61], A. White[78], D. Wicke[25], M.R.J. Williams[43], G.W. Wilson[58], S.J. Wimpenny[48], M. Wobisch[60], D.R. Wood[63], T.R. Wyatt[45], Y. Xie[77], C. Xu[64], S. Yacoob[53], R. Yamada[50], W.-C. Yang[45], T. Yasuda[50], Y.A. Yatsunenko[37], Z. Ye[50], H. Yin[7], K. Yip[73], H.D. Yoo[77], S.W. Youn[50], J. Yu[78], C. Zeitnitz[27], S. Zelitch[81], T. Zhao[82], B. Zhou[64], J. Zhu[72], M. Zielinski[71], D. Zieminska[54], L. Zivkovic[70], V. Zutshi[52], and E.G. Zverev[39]

(The DØ Collaboration)

[1] Universidad de Buenos Aires, Buenos Aires, Argentina
[2] LAFEX, Centro Brasileiro de Pesquisas Físicas, Rio de Janeiro, Brazil
[3] Universidade do Estado do Rio de Janeiro, Rio de Janeiro, Brazil
[4] Universidade Federal do ABC, Santo André, Brazil
[5] Instituto de Física Teórica, Universidade Estadual Paulista, São Paulo, Brazil
[6] University of Alberta, Edmonton, Alberta, Canada; Simon Fraser University, Burnaby, British Columbia, Canada; York University, Toronto, Ontario, Canada and McGill University, Montreal, Quebec, Canada
[7] University of Science and Technology of China, Hefei, People's Republic of China
[8] Universidad de los Andes, Bogotá, Colombia
[9] Center for Particle Physics, Charles University, Faculty of Mathematics and Physics, Prague, Czech Republic
[10] Czech Technical University in Prague, Prague, Czech Republic
[11] Center for Particle Physics, Institute of Physics, Academy of Sciences of the Czech Republic, Prague, Czech Republic
[12] Universidad San Francisco de Quito, Quito, Ecuador
[13] LPC, Université Blaise Pascal, CNRS/IN2P3, Clermont, France
[14] LPSC, Université Joseph Fourier Grenoble 1, CNRS/IN2P3, Institut National Polytechnique de Grenoble, Grenoble, France
[15] CPPM, Aix-Marseille Université, CNRS/IN2P3, Marseille, France
[16] LAL, Université Paris-Sud, IN2P3/CNRS, Orsay, France
[17] LPNHE, IN2P3/CNRS, Universités Paris VI and VII, Paris, France
[18] CEA, Irfu, SPP, Saclay, France
[19] IPHC, Université de Strasbourg, CNRS/IN2P3, Strasbourg, France
[20] IPNL, Université Lyon 1, CNRS/IN2P3, Villeurbanne, France and Université de Lyon, Lyon, France
[21] III. Physikalisches Institut A, RWTH Aachen University, Aachen, Germany
[22] Physikalisches Institut, Universität Bonn, Bonn, Germany
[23] Physikalisches Institut, Universität Freiburg, Freiburg, Germany
[24] II. Physikalisches Institut, Georg-August-Universität Göttingen, Göttingen, Germany
[25] Institut für Physik, Universität Mainz, Mainz, Germany
[26] Ludwig-Maximilians-Universität München, München, Germany
[27] Fachbereich Physik, University of Wuppertal, Wuppertal, Germany
[28] Panjab University, Chandigarh, India
[29] Delhi University, Delhi, India
[30] Tata Institute of Fundamental Research, Mumbai, India
[31] University College Dublin, Dublin, Ireland
[32] Korea Detector Laboratory, Korea University, Seoul, Korea
[33] SungKyunKwan University, Suwon, Korea
[34] CINVESTAV, Mexico City, Mexico
[35] FOM-Institute NIKHEF and University of Amsterdam/NIKHEF, Amsterdam, The Netherlands
[36] Radboud University Nijmegen/NIKHEF, Nijmegen, The Netherlands
[37] Joint Institute for Nuclear Research, Dubna, Russia
[38] Institute for Theoretical and Experimental Physics, Moscow, Russia
[39] Moscow State University, Moscow, Russia
[40] Institute for High Energy Physics, Protvino, Russia

^{41}*Petersburg Nuclear Physics Institute, St. Petersburg, Russia*
^{42}*Stockholm University, Stockholm, Sweden, and Uppsala University, Uppsala, Sweden*
^{43}*Lancaster University, Lancaster, United Kingdom*
^{44}*Imperial College, London, United Kingdom*
^{45}*University of Manchester, Manchester, United Kingdom*
^{46}*University of Arizona, Tucson, Arizona 85721, USA*
^{47}*California State University, Fresno, California 93740, USA*
^{48}*University of California, Riverside, California 92521, USA*
^{49}*Florida State University, Tallahassee, Florida 32306, USA*
^{50}*Fermi National Accelerator Laboratory, Batavia, Illinois 60510, USA*
^{51}*University of Illinois at Chicago, Chicago, Illinois 60607, USA*
^{52}*Northern Illinois University, DeKalb, Illinois 60115, USA*
^{53}*Northwestern University, Evanston, Illinois 60208, USA*
^{54}*Indiana University, Bloomington, Indiana 47405, USA*
^{55}*University of Notre Dame, Notre Dame, Indiana 46556, USA*
^{56}*Purdue University Calumet, Hammond, Indiana 46323, USA*
^{57}*Iowa State University, Ames, Iowa 50011, USA*
^{58}*University of Kansas, Lawrence, Kansas 66045, USA*
^{59}*Kansas State University, Manhattan, Kansas 66506, USA*
^{60}*Louisiana Tech University, Ruston, Louisiana 71272, USA*
^{61}*University of Maryland, College Park, Maryland 20742, USA*
^{62}*Boston University, Boston, Massachusetts 02215, USA*
^{63}*Northeastern University, Boston, Massachusetts 02115, USA*
^{64}*University of Michigan, Ann Arbor, Michigan 48109, USA*
^{65}*Michigan State University, East Lansing, Michigan 48824, USA*
^{66}*University of Mississippi, University, Mississippi 38677, USA*
^{67}*University of Nebraska, Lincoln, Nebraska 68588, USA*
^{68}*Princeton University, Princeton, New Jersey 08544, USA*
^{69}*State University of New York, Buffalo, New York 14260, USA*
^{70}*Columbia University, New York, New York 10027, USA*
^{71}*University of Rochester, Rochester, New York 14627, USA*
^{72}*State University of New York, Stony Brook, New York 11794, USA*
^{73}*Brookhaven National Laboratory, Upton, New York 11973, USA*
^{74}*Langston University, Langston, Oklahoma 73050, USA*
^{75}*University of Oklahoma, Norman, Oklahoma 73019, USA*
^{76}*Oklahoma State University, Stillwater, Oklahoma 74078, USA*
^{77}*Brown University, Providence, Rhode Island 02912, USA*
^{78}*University of Texas, Arlington, Texas 76019, USA*
^{79}*Southern Methodist University, Dallas, Texas 75275, USA*
^{80}*Rice University, Houston, Texas 77005, USA*
^{81}*University of Virginia, Charlottesville, Virginia 22901, USA and*
^{82}*University of Washington, Seattle, Washington 98195, USA*
(Dated: November 4, 2009)

We present a search for charged Higgs bosons in top quark decays. We analyze the e+jets, μ+jets, ee, $e\mu$, $\mu\mu$, τe and $\tau\mu$ final states from top quark pair production events, using data from about 1 fb^{-1} of integrated luminosity recorded by the D0 experiment at the Fermilab Tevatron Collider. We consider different scenarios of possible charged Higgs boson decays, one where the charged Higgs boson decays purely hadronically into a charm and a strange quark, another where it decays into a τ lepton and a τ neutrino and a third one where both decays appear. We extract limits on the branching ratio $B(t \to H^+b)$ for all these models. We use two methods, one where the $t\bar{t}$ production cross section is fixed, and one where the cross section is fitted simultaneously with $B(t \to H^+b)$. Based on the extracted limits, we exclude regions in the charged Higgs boson mass and $\tan\beta$ parameter space for different scenarios of the minimal supersymmetric standard model.

I. INTRODUCTION

In many extensions of the standard model (SM), including supersymmetry (SUSY) and grand unified theories, the existence of an additional Higgs doublet is required. Such models predict multiple physical Higgs particles, including three neutral and two charged Higgs bosons ($H^{\pm}$) [1]. If the charged Higgs boson is sufficiently light, it can appear in top quark decays $t \to H^+b$ [2].

Within the SM, the top quark decay into a W boson and a b quark occurs with almost 100% probability. The

$t\bar{t}$ final state signatures are fully determined by the W boson decay modes. Measurements of top quark pair production cross sections $\sigma_{t\bar{t}}$ in various channels [3] are potentially sensitive to the decay of top quarks to charged Higgs bosons. The presence of a light charged Higgs boson would result in a different distribution of $t\bar{t}$ events between different final states than expected in the SM.

In this Letter we compare the number of predicted and observed events in various $t\bar{t}$ final states and derive 95% confidence level (CL) limits on the production of charged Higgs bosons from top quark decays. The analysis is based on data collected with the D0 detector between August 2002 and February 2006 at the Fermilab Tevatron $p\bar{p}$ Collider at $\sqrt{s} = 1.96$ TeV. The analyzed datasets correspond to an integrated luminosity of about 1 fb^{-1}.

The decay modes of the charged Higgs boson depend on the ratio of the vacuum expectation values of the two Higgs doublets, $\tan\beta$. For small values of $\tan\beta$ it is dominated by the decay to quarks, while for larger values of $\tan\beta$ it is dominated by the decay to a τ lepton and a neutrino. We consider three models for the charged Higgs boson decay: a purely leptophobic model, where the charged Higgs boson decays into a charm and a strange quark, a purely tauonic model, where the charged Higgs boson decays exclusively into a τ lepton and a neutrino, and a model where both decays can occur. In all models we fix the $t\bar{t}$ cross section to the theoretical value within the SM and extract $B(t \to H^+b)$. In the case of the tauonic model, in addition we extract $\sigma_{t\bar{t}}$ and $B(t \to H^+b)$ simultaneously, thus yielding a limit without assuming a particular value of the $t\bar{t}$ cross section.

A scenario in which the charged Higgs boson decays exclusively into quarks can be realized, for instance, in a general multi-Higgs-doublet model (MHDM) [4]. It has been demonstrated that such leptophobic charged Higgs bosons with a mass of about 80 GeV could lead to noticeable effects at the Tevatron if $\tan\beta \leq 3.5$ [5]. Moreover, large radiative corrections from SUSY-breaking effects can lead to a suppression of $H^+ \to \tau^+\nu$ compared to $H^+ \to c\bar{s}$ [6]. In that case, for small $\tan\beta$, hadronic charged Higgs decays can become large in both the two-Higgs-doublet (2HDM) [5] and the minimal supersymmetric standard model (MSSM).

For values of $\tan\beta \geq 20$ we consider different models leading to different branching ratios. Values of $B(H^+ \to c\bar{s})$ close to one are predicted in specific CP-violating benchmark scenarios (CPX) with large threshold corrections [7]. For other models, the tauonic decays of the charged Higgs boson dominate at high $\tan\beta$, for example, in the $m_h^{\max}$ benchmark scenario [8] where $B(H^+ \to \tau^+\nu)$ can be close to one.

II. EVENT SELECTION AND ANALYSIS METHOD

This search for charged Higgs bosons is based on the following $t\bar{t}$ final states: the dilepton ($\ell\ell$) channel where

both charged bosons (W^+ or H^+) decay into a light charged lepton ($\ell = e$ or μ) either directly or through the leptonic decay of a τ, the τ+lepton ($\tau\ell$) channel where one charged boson decays to a light charged lepton and the other one to a τ-lepton decaying hadronically, and the lepton plus jets (ℓ+jets) channel where one charged boson decays to a light charged lepton and the other decays into hadrons. We select events to create 14 subchannels: (i) ee ($\mu\mu$) subchannel with two isolated high transverse momentum (p_T) electrons (muons) and at least two high p_T jets; (ii) $e\mu$ subchannels with one isolated high p_T electron and one muon and exactly one or at least two jets; (iii) τe ($\tau\mu$) subchannel with one high p_T hadronically decaying τ, one electron (muon) and at least two high p_T jets one of which is identified as a b jet; (iv) ℓ+jets subchannels with one isolated high p_T electron (muon), exactly three or at least four high p_T jets, further split into subsamples with one or at least two b-tagged jets. Details of the event selection and object reconstruction in the dilepton and $\tau\ell$ channels can be found in Ref. [9]; a more detailed description of the ℓ+jets channel and the combination are given in Ref. [3]. All event samples are constructed to be mutually exclusive.

In the ℓ+jets channel the main background consists of W+jets production, with smaller contributions from multijet, single top quark and diboson production. The background contribution in the $\tau\ell$ channel is dominated by multijet events, while the most important background in the $\ell\ell$ channel emerges from Z+jets production. The sample composition of all 14 subchannels, assuming $B(t \to W^+b) = 1$ (hence $B(t \to H^+b)$=0), is given in Ref. [3].

The simulation of the W+jets and Z+jets backgrounds as well as the $t\bar{t}$ signal with no charged Higgs boson decay is performed using ALPGEN [10] for the matrix element calculation, followed by PYTHIA [11] for parton showering and hadronization. Diboson samples are generated using PYTHIA, while single top quark events are simulated using the SINGLETOP [12] generator. The generated events are processed through a GEANT-based [13] simulation of the D0 detector and the same reconstruction programs used for the data.

We simulate the signal containing charged Higgs bosons with the PYTHIA Monte Carlo event generator [11], separately for the decays $t\bar{t} \to W^+bH^-\bar{b}$ (and its charge conjugate) and $t\bar{t} \to H^+bH^-\bar{b}$. The total signal selection efficiency is calculated as a function of $B \equiv B(t \to H^+b)$ as given by:

$$\epsilon_{t\bar{t}} = (1-B)^2 \cdot \epsilon_{t\bar{t}\to W^+bW^-\bar{b}} + 2B(1-B) \cdot \epsilon_{t\bar{t}\to W^+bH^-\bar{b}} + B^2 \cdot \epsilon_{t\bar{t}\to H^+bH^-\bar{b}}, \tag{1}$$

yielding the number of $t\bar{t}$ events as a function of B. The efficiencies $\epsilon_{t\bar{t}\to W^+bH^-\bar{b}}$ and $\epsilon_{t\bar{t}\to H^+bH^-\bar{b}}$ are evaluated for the assumed H^+ decay modes. Figure 1 shows the number of expected events for different values of $B(t \to H^+b)$ assuming $M_{H^+} = 80$ GeV and either $B(H^+ \to c\bar{s}) = 1$ or $B(H^+ \to \tau^+\nu) = 1$, compared to the number of observed events in the considered channels. The ℓ+jets en-
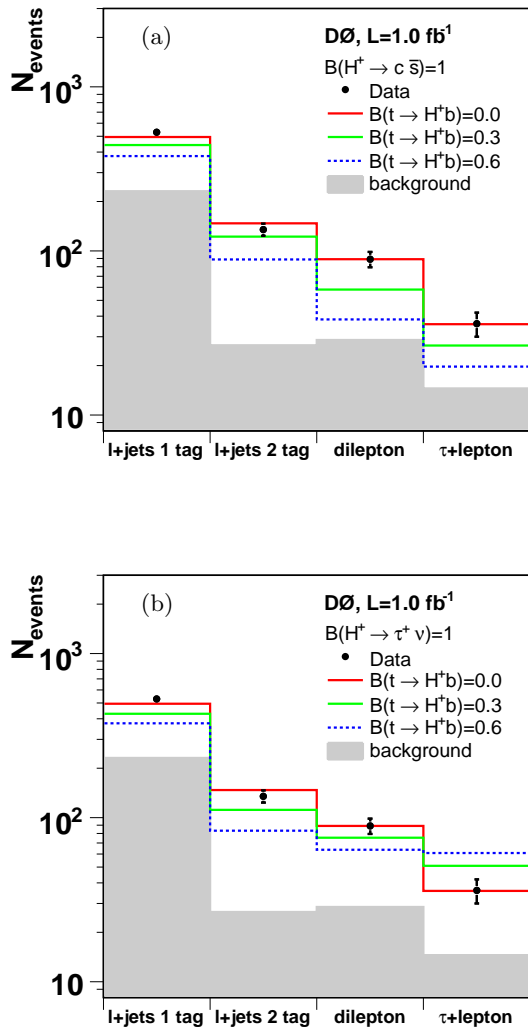
FIG. 1: Number of expected and observed events versus final state for $M_{H^+} = 80$ GeV assuming either exclusive $\tau^+\nu$ (a) or exclusive $c\bar{s}$ (b) decays of the charged Higgs boson.

tries with one and two b-tags represent the sum of four ℓ+jets subchannels each (with different light lepton flavor and $= 3$ and ≥ 4 jets). The dilepton contribution corresponds to the sum of the ee, $\mu\mu$ and two $e\mu$ subchannels, and the τ+lepton one shows the sum of the τe and $\tau\mu$ subchannels. For a non-zero branching ratio $B(t \to H^+b \to c\bar{s}b)$ the number of events decreases in the ℓ+jets, $\ell\ell$ and $\tau\ell$ final states. In case of a non-zero branching ratio $B(t \to H^+b \to \tau^+\nu b)$ the number of predicted events increases in the $\tau\ell$ channel while it decreases in all other channels. The latter are often called disappearance channels.

III. EXTRACTION OF LIMITS ON $B(t \to H^+b)$

The extraction of $B(t \to H^+b)$ is done by calculating the predicted number of events in 14 search subchannels for various charged Higgs boson masses and branching ratios, and performing a maximum likelihood fit to the number of observed events in data. We constrain the multijet background determined from control samples in the ℓ+jets and $\tau\ell$ channels by including Poisson terms in the likelihood function. We account for systematic uncertainties in the fit by modeling each independent source of systematic uncertainty as a Gaussian probability density function $\mathcal{G}$ with zero mean and width corresponding to one standard deviation (SD) of the parameter representing the systematic uncertainty. Correlations of systematic uncertainties between channels are naturally taken into account by using the same parameter for the same source of systematic uncertainty. The parameter for each systematic uncertainty is allowed to float during the likelihood fit. We maximize the likelihood function

$$\mathcal{L} = \prod_{i=1}^{14} \mathcal{P}(n_i, m_i) \times \prod_{j=1}^{14} \mathcal{P}(n_j, m_j) \times \prod_{k=1}^{K} \mathcal{G}(\nu_k; 0, \mathrm{SD}),$$

(2)

with $\mathcal{P}(n, m)$ representing the Poisson probability to observe n events when m events are expected. The product runs over the subsamples i, and multijet background samples j. K is the total number of independent sources of systematic uncertainty, with ν_k being the corresponding nuisance parameter. The predicted number of events in each channel is the sum of the predicted background and the expected $t\bar{t}$ events, which depends on $B(t \to H^+b)$.

During the fit, the $t\bar{t}$ cross section is set to $7.48^{+0.55}_{-0.72}$ pb, corresponding to an approximation to the next-to-next-to-leading-order (NNLO) QCD cross section that includes all next-to-next-to-leading logarithms (NNLL) relevant in NNLO QCD [14] at the world average top quark mass of 173.1 GeV [15]. The uncertainty on the theoretical cross section includes the uncertainty on the world average top quark mass.

Since we find no evidence for a charged Higgs boson, we extract upper limits on $B(t \to H^+b)$, assuming that $B(H^+ \to c\bar{s}) = 1$, or $B(H^+ \to \tau^+\nu) = 1$, or a mixture of both. The limit setting procedure follows the likelihood ratio ordering principle of Feldman and Cousins [16]. The determination of the limits requires the generation of pseudo-datasets. We generate ensembles of 10,000 pseudo-datasets with $B(t \to H^+b)$ varied between zero and one in steps of 0.05, fully taking into account the systematic uncertainties and their correlations.

Table I shows an example of the uncertainties on $B(t \to H^+b)$ for $M_{H^+} = 80$ GeV in the tauonic and leptophobic charged Higgs boson models. We consider systematic uncertainties originating from electron, muon, τ and jet identification, τ and jet energy calibration, b-jet identification, limited statistics of data or Monte Carlo samples, modeling of triggers, signal and background,

and integrated luminosity. To evaluate the signal modeling uncertainty we replace the SM $t\bar{t}$ sample generated with ALPGEN by the one generated with PYTHIA and take the difference in acceptance as systematic uncertainty. For both the tauonic and leptophobic model, the two main sources of systematic uncertainty on $B(t \to H^+b)$ are the uncertainty on the luminosity of 6.1% and the $t\bar{t}$ cross section, followed by the non-negligible uncertainties on signal modeling, b jet identification and jet energy scale. The former two are approximately of the same size as the statistical uncertainty. Since in the tauonic model we consider both appearance and disappearance channels, some uncertainties affecting the signal and background normalization cancel. Therefore, uncertainties on signal modeling, the $t\bar{t}$ cross section, lepton identification and luminosity are reduced in the tauonic model compared to the leptophobic model.

TABLE I: Uncertainties on $B(t \to H^+b)$ for the leptophobic and tauonic model, assuming $M_{H^+} = 80$ GeV.

	leptophobic		tauonic	
Source	+1 SD	−1 SD	+1 SD	−1 SD
Statistical uncertainty	0.057	-0.058	0.047	−0.046
Lepton identification	0.017	-0.017	0.010	−0.010
Tau identification	0.004	-0.004	0.006	−0.006
Jet identification	0.009	-0.009	0.010	−0.010
b jet identification	0.031	-0.030	0.030	−0.030
Jet energy scale	0.016	-0.019	0.020	−0.020
Tau energy scale	0.004	-0.004	0.004	−0.004
Trigger modeling	0.007	-0.011	0.007	−0.006
Signal modeling	0.023	-0.024	0.010	−0.010
Background estimation	0.013	-0.014	0.011	−0.010
Multijet background	0.014	-0.016	0.019	−0.017
$\sigma_{t\bar{t}}$	0.059	-0.085	0.040	−0.054
Luminosity	0.056	-0.060	0.035	−0.036
Other	0.017	-0.017	0.010	−0.010
Total systematic uncertainty	0.097	-0.118	0.071	−0.079

TABLE II: Expected and observed upper limits on the branching ratio $B(t \to H^+b)$ for each generated H^+ mass.

	leptophobic		tauonic		tauonic from simultaneous fit		
M_{H^+} (GeV)	exp	obs	exp	obs	exp	obs	$\sigma_{t\bar{t}}$ (pb)
80	0.25	0.21	0.18	0.16	0.14	0.13	$8.07^{+1.17}_{-1.04}$
100	0.25	0.22	0.17	0.15	0.13	0.12	$8.11^{+1.13}_{-1.00}$
120	0.25	0.22	0.18	0.17	0.15	0.14	$8.12^{+1.20}_{-1.05}$
140	0.24	0.21	0.19	0.18	0.18	0.19	$8.26^{+1.39}_{-1.20}$
150	0.22	0.20	0.19	0.19	0.21	0.25	$8.63^{+1.65}_{-1.38}$
155	0.22	0.19	0.19	0.18	0.24	0.26	$8.49^{+1.75}_{-1.45}$

Figure 2 shows the expected and observed upper limits on $B(t \to H^+b)$ assuming $B(H^+ \to c\bar{s}) = 1$ or $B(H^+ \to \tau^+\nu) = 1$ as a function of M_{H^+} along with the one standard deviation band around the expected limit. Table II lists the corresponding expected and observed
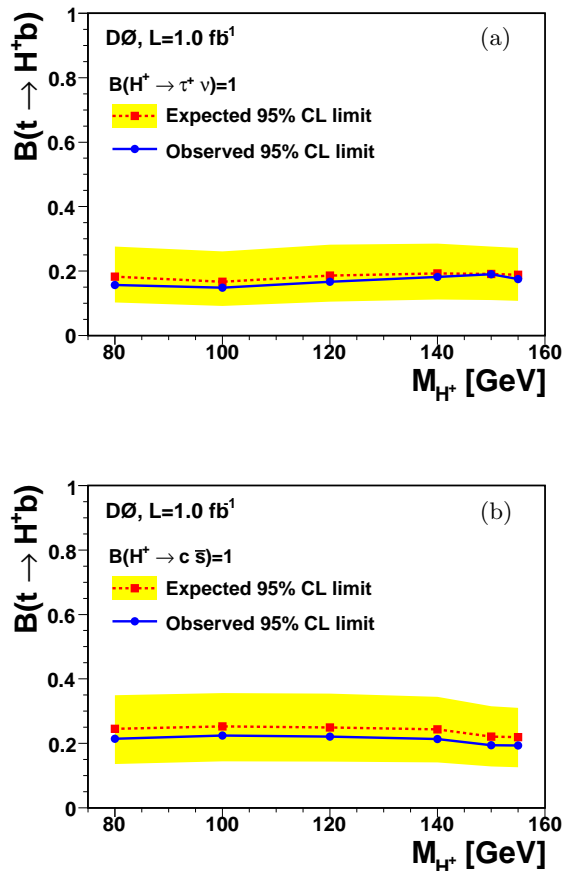

FIG. 2: Upper limit on $B(t \to H^+b)$ for the tauonic (a) and leptophobic (b) model versus M_{H^+}. The yellow band shows the ± 1 SD band around the expected limit (Color version online).

upper limits on $B(t \to H^+b)$ for each generated M_{H^+}. In the tauonic model we exclude $B(t \to H^+b) > 0.15 - 0.19$ and $B(t \to H^+b) > 0.19 - 0.22$ in the leptophobic case.

The CDF Collaboration reported a search for charged Higgs bosons using different $t\bar{t}$ decay channels with a data set of about 200 pb^{-1} [17], resulting in $B(t \to H^+b) < 0.4$ within the tauonic model. Recently, D0 reported limits on $B(t \to H^+b)$ for the tauonic and leptophobic models extracted from cross section ratios [3] and for the tauonic model based on a measurement of the $t\bar{t}$ cross section in ℓ+jets channel using topological event information [18]. Exploring the full set of channels as presented here improves the limits derived in the cross section ratio method for the leptophobic and for the tauonic model in the high M_{H^+} region.

We also extract upper limits on $B(t \to H^+b)$ mixing the tauonic and leptophobic models under the assumption $B(H^+ \to \tau^+\nu) + B(H^+ \to c\bar{s}) = 1$. We repeat the extraction of upper limits on $B(t \to H^+b)$ in the range of $0 \leq B(H^+ \to \tau^+\nu) \leq 1$ in steps of 0.1. For each assumed M_{H^+} we parametrize the expected and observed limits dependent on the mixture between tauonic

and leptophobic decays. Figure 3 shows upper limits on $B(t \to H^+b)$ as a function of $B(H^+ \to c\bar{s})$. As expected, the upper limit decreases with increasing tauonic decay fraction.

IV. SIMULTANEOUS EXTRACTION OF $B(t \to H^+b)$ AND $\sigma_{t\bar{t}}$

The search for charged Higgs bosons in top quark decays is based on the distribution of $t\bar{t}$ events between the various final states. Naturally, it is also sensitive to the total number of $t\bar{t}$ events. This results in a large systematic uncertainty due to the theoretical uncertainty in the $t\bar{t}$ cross section calculations. If $\sigma_{t\bar{t}}$ and $B(t \to H^+b)$ are measured simultaneously the limit becomes independent of the assumed theoretical $t\bar{t}$ cross section. Furthermore, the luminosity uncertainty and other systematic uncertainties affecting the signal normalization are partially absorbed by the fitted cross section.

We perform a simultaneous fit of $\sigma_{t\bar{t}}$ and $B(t \to H^+b)$ for the tauonic model. The fitting and limit setting procedure is the same as described in Sec. III, with two free parameters instead of one. Table III shows the uncertainties on $B(t \to H^+b)$ and $\sigma_{t\bar{t}}$ for $M_{H^+} = 80$ GeV. The correlation between the two fitted quantities is about 70% for M_{H^+} up to 130 GeV and it reaches 90% for $M_{H^+} = 155$ GeV. For high charged Higgs boson masses, where the correlation becomes high, the sensitivity degrades compared to the case where the $t\bar{t}$ cross section is fixed.

The $t\bar{t}$ cross section is set to the measured value in the generation of pseudo-datasets for the limit setting procedure. For the fit to the pseudo-data, $\sigma_{t\bar{t}}$ and $B(t \to H^+b)$ are allowed to float. In Table II the expected and observed upper limits on $B(t \to H^+b)$ are listed together with the simultaneous measurement of the $t\bar{t}$ cross section for a top quark mass of 170 GeV. Within uncertainties, the obtained cross section for all masses of the charged Higgs boson agrees with $\sigma_{t\bar{t}} = 8.18^{+0.98}_{-0.87}$ pb, which was measured on the same data set assuming $B(t \to W^+b) = 1$ [3].

In Fig. 4 the upper limits on $B(t \to H^+b)$ for M_{H^+} from 80 to 155 GeV are shown. For small M_{H^+}, the simultaneous fit provides an improvement of the sensitivity of more than 20% compared to the case where the $t\bar{t}$ cross section is fixed. Furthermore, the $t\bar{t}$ cross section measured here represents a measurement independent of the assumption $B(t \to W^+b) = 1$.

The simultaneous fit requires a reasonably small correlation between the two fitted observables. Since at present we have only included disappearance channels for the leptophobic model, the correlation between $B(t \to H^+b)$ and $\sigma_{t\bar{t}}$ is large ($\approx 90\%$) for all charged Higgs boson masses, and thus we have not used the simultaneous fit method there.

TABLE III: Uncertainties on $B(t \to H^+b)$ and $\sigma_{t\bar{t}}$ for the simultaneous fit in the tauonic model, assuming $M_{H^+} = 80$ GeV.

	$B(t \to H^+b)$		$\sigma_{t\bar{t}}$	(pb)
Source	+1 SD	−1 SD	+1 SD	−1 SD
Statistical uncertainty	0.067	-0.066	0.68	-0.64
Lepton identification	0.001	-0.001	0.16	-0.13
Tau identification	0.014	-0.014	0.12	-0.13
Jet identification	0.005	-0.005	0.07	-0.07
b jet identification	0.003	-0.003	0.31	-0.29
Jet energy scale	0.014	-0.014	0.10	-0.09
Tau energy scale	0.011	-0.010	0.10	-0.08
Trigger modeling	0.009	-0.000	0.12	-0.11
Signal modeling	0.014	-0.016	0.23	-0.23
Background estimation	0.003	-0.003	0.15	-0.14
Multijet background	0.036	-0.033	0.31	-0.34
Luminosity	0.002	-0.002	0.57	-0.48
Other	0.006	-0.006	0.17	-0.17
Total systematic uncertainty	0.047	-0.044	0.84	-0.77

V. INTERPRETATIONS IN SUPERSYMMETRIC MODELS

The limits on $B(t \to H^+b)$ presented in Figs. 2, 3 and 4 are interpreted in different SUSY models and excluded regions of $[\tan\beta, M_{H^+}]$ parameter space are derived. The investigated MSSM benchmark models [8] depend on several model parameters: μ is the strength of the supersymmetric Higgs boson mixing; $M_{\rm SUSY}$ is a soft SUSY-breaking mass parameter representing a common mass for all scalar fermions (sfermions) at the electroweak scale; $A = A_t = A_b$ is a common trilinear Higgs-squark coupling at the electroweak scale; $X_t = A - \mu \cot\beta$ is the stop mixing parameter; M_2 denotes a common SU(2) gaugino mass at the electroweak scale; and M_3 is the gluino mass. The top quark mass, which has a significant impact on the calculations through radiative corrections, is set to the current world average of 173.1 GeV [15].

Direct searches for charged Higgs bosons have been performed by the LEP experiments resulting into limits of $M_{H^+} < 79.3$ GeV in the framework of 2HDM [19]. Indirect bounds on M_{H^+} in the region of $\tan\beta < 40$ were obtained for several MSSM scenarios [20], two of which are identical to the ones presented in Sect. V C and V D of this Letter.

A. Leptophobic model

A leptophobic model with a branching ratio of $B(H^+ \to c\bar{s}) = 1$ is possible in MHDM [4, 5]. Here we calculate the branching ratio $B(t \to H^+b)$ as a function of $\tan\beta$, and the charged Higgs boson mass including higher order QCD corrections [21] using FEYNHIGGS [22].

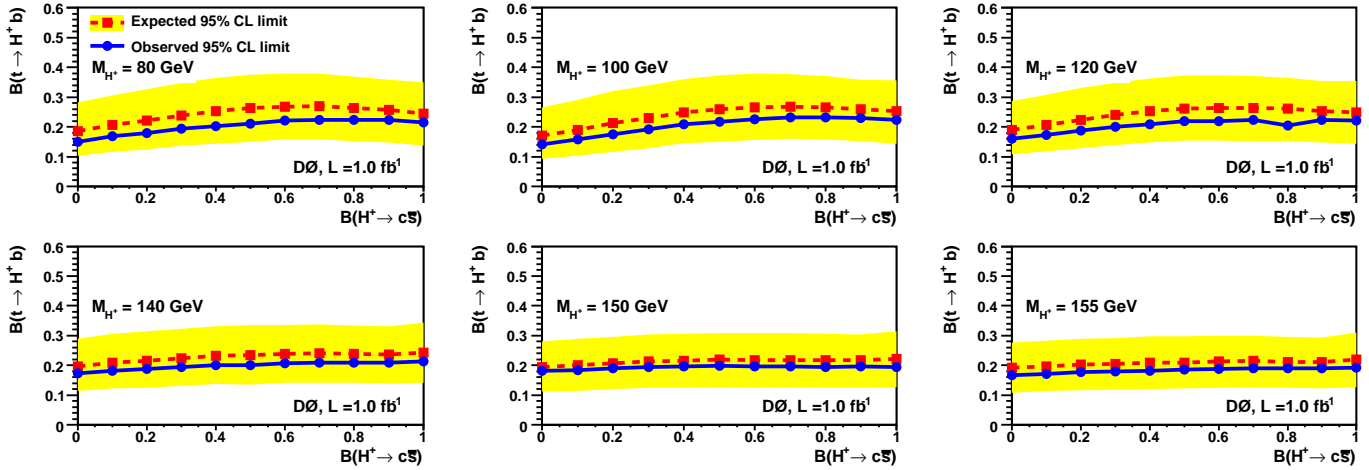FIG. 3: Upper limits on $B(t \to H^+ b)$ parametrized as function of $B(H^+ \to c\bar{s})$ for different assumed M_{H^+}. The yellow band shows the ± 1 SD band around the expected limit (Color version online).
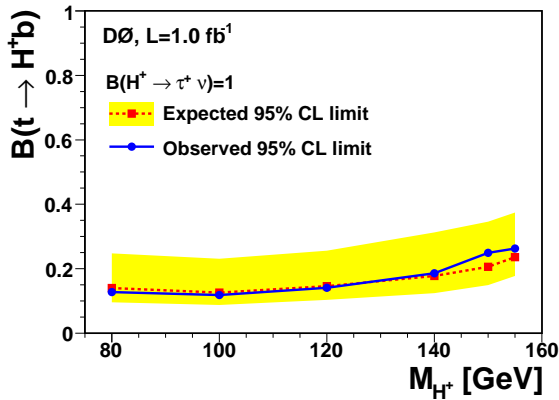

FIG. 4: Upper limit on $B(t \to H^+ b)$ for the simultaneous fit of $B(t \to H^+ b)$ and $\sigma_{t\bar{t}}$ versus M_{H^+}. The yellow band shows the ± 1 SD band around the expected limit (Color version online).

TABLE IV: Summary of the most important SUSY parameter values (in GeV) for different MSSM benchmark scenarios.

parameter	$\mathrm{CPX_{gh}}$	m_h-max	no-mixing
μ	2000	200	200
M_{SUSY}	500	1000	2000
A	$1000 \cdot \exp(i\pi/2)$		
X_t		2000	0
M_2	200	200	200
M_3	$1000 \cdot \exp(i\pi)$	800	1600

Figure 5 shows the excluded region of $[\tan\beta, M_{H^+}]$ parameter space. For $\tan\beta = 0.5$, for example, M_{H^+} up to 153 GeV are excluded. For low M_{H^+}, values of $\tan\beta$ up to 1.7 are excluded. These are the most stringent limits on the $[\tan\beta, M_{H^+}]$ plane in leptophobic charged Higgs boson models to date.

B. CPX model with generation hierarchy

$B(H^+ \to \tau^+ \nu) + B(H^+ \to c\bar{s}) \approx 1$ can be realized in a particular CPX benchmark scenario ($\mathrm{CPX_{gh}}$) [7] of the MSSM. This scenario is identical to the CPX scenario investigated in [20] except for a different choice of $\arg(A)$ and an additional mass hierarchy between the first two and the third generation of sfermions which is introduced as follows:

$$M_{\tilde{X}_{1,2}} = \rho_{\tilde{X}} M_{\tilde{X}_3}, \qquad (3)$$

where $\tilde{X}$ collectively represents the chiral multiplet for the left-handed doublet squarks $\tilde{Q}$, the right-handed up-type (down-type) squarks $\tilde{U}$ ($\tilde{D}$), the left-handed doublet sleptons $\tilde{L}$ or the right-handed charged sleptons $\tilde{E}$. Taking $\rho_{\tilde{U},\tilde{L},\tilde{E}} = 1$, $\rho_{\tilde{Q},\tilde{D}} = 0.4$ and requiring that the masses of the scalar left- and right-handed quarks and leptons
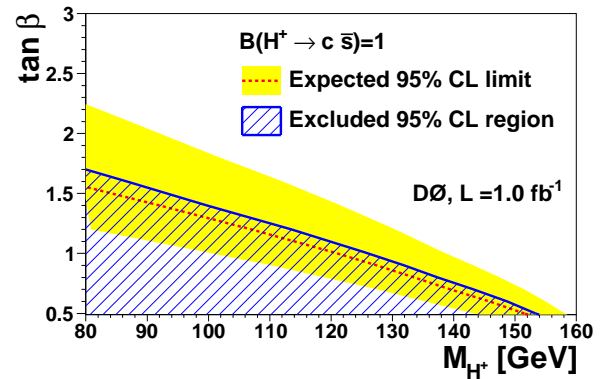

FIG. 5: Excluded regions of $[\tan\beta, M_{H^+}]$ parameter space for leptophobic model. The yellow band shows the ± 1 SD band around the expected limit (Color version online).
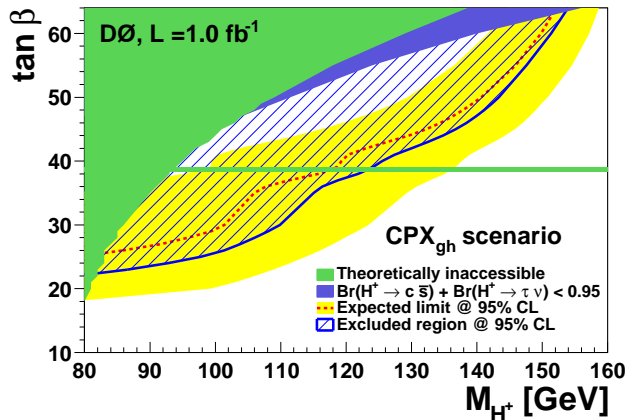
8

FIG. 6: Excluded region of $[\tan\beta, M_{H^+}]$ parameter space in the MSSM for the CPX_{gh} scenario with generation hierarchy such that $B(H^+ \to c\bar{s}) + B(H^+ \to \tau^+\nu) \approx 1$. The yellow band shows the ± 1 SD band around the expected limit (Color version online).

FIG. 7: Excluded region of $[\tan\beta, M_{H^+}]$ parameter space in the MSSM for the no-mixing scenario. The yellow band shows the ± 1 SD band around the expected limit (Color version online).

are large $M_{\tilde{Q}_3,\tilde{D}_3} = 2M_{\tilde{U}_3,\tilde{L}_3,\tilde{E}_3} = 2$ TeV, we calculate the branching ratios $B(t \to H^+ b)$ including higher order QCD and higher order MSSM corrections using the CPX_{gh} MSSM parameters in Table IV. The calculation is performed with the program CPSUPERH [23]. Figure 6 shows the excluded region in the $[\tan\beta, M_{H^+}]$ parameter space. Theoretically inaccessible regions indicate parts of the parameter space where perturbative calculations cannot be performed reliably. In the $[\tan\beta, M_{H^+}]$ region analyzed here, the sum of the branching ratios was found to be $B(H^+ \to \tau^+\nu) + B(H^+ \to c\bar{s}) > 0.99$ except for values very close to the blue region which indicates $B(H^+ \to \tau^+\nu) + B(H^+ \to c\bar{s}) < 0.95$. The charged Higgs decay $H^+ \to \tau^+\nu$ dominates for $\tan\beta$ below 22 and above 55. For the rest of the $[\tan\beta, M_{H^+}]$ parameter space both the hadronic and the tauonic decays of charged Higgs bosons are important. In the region $38 \le \tan\beta \le 40$, the hadronic decays of the charged Higgs boson dominate and $B(H^+ \to c\bar{s}) > 0.95$. For large values of $\tan\beta$, M_{H^+} up to 154 GeV are excluded. For low charged Higgs masses, $\tan\beta$ values down to 23 are excluded. These are the first Tevatron limits on a CP-violating MSSM scenario derived from the charged Higgs sector.

C. No-mixing scenario

In the CP-conserving no-mixing scenario, the stop mixing parameter X_t is set to zero, giving rise to a relatively restricted MSSM parameter space. In the $[\tan\beta, M_{H^+}]$ parameter space analyzed here the branching ratio is $B(H^+ \to \tau^+\nu) > 0.99$ except for very low values of $\tan\beta$ and M_{H^+} where $B(H^+ \to \tau^+\nu) > 0.95$. We interpret the results derived in the tauonic model using the simultaneous fit in the framework of the no-mixing sce-

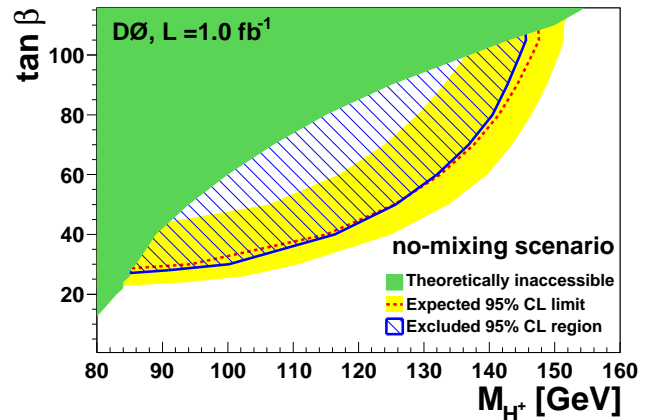nario. The branching ratios $B(t \to H^+ b)$ are calculated including higher order QCD and higher order MSSM corrections using the no-mixing MSSM parameters as given in Table IV. The calculation is performed with FEYN-HIGGS [22]. Figure 7 presents the excluded region of $[\tan\beta, M_{H^+}]$ parameter space. For large values of $\tan\beta$, M_{H^+} up to 145 GeV are excluded. For low M_{H^+}, values of $\tan\beta$ down to 27 are excluded.

D. m_h-max scenario

In the CP-conserving m_h-max scenario the stop mixing parameter is set to a large value, $X_t = 2M_{SUSY}$. The theoretical upper bound on the lighter CP-even neutral scalar, m_h, for a given value of $\tan\beta$ and fixed m_t and M_{SUSY} is designed to be maximal. Therefore the model provides the largest parameter space in m_h and as a consequence, less restrictive exclusion limits on $\tan\beta$ than the other models. In the investigated $[\tan\beta, M_{H^+}]$ parameter space, $B(H^+ \to \tau^+\nu) > 0.99$ holds except for low values of $\tan\beta$ and M_{H^+}, where $B(H^+ \to \tau^+\nu) > 0.97$. Thus we use the simultaneous fit results within the tauonic model to derive constraints on the m_h-max scenario. The branching ratios $B(t \to H^+ b)$ are calculated using FEYNHIGGS [22] including higher order QCD and higher order MSSM corrections. The m_h-max MSSM parameters are given in Table IV.

Figure 8 shows the excluded region of $[\tan\beta, M_{H^+}]$ parameter space. For large values of $\tan\beta$, M_{H^+} up to 149 GeV are excluded. These are the most stringent limits from the Tevatron to date. For low charged Higgs boson masses, values of $\tan\beta$ down to 29 are excluded.

9

VI. SUMMARY

We have performed a search for charged Higgs bosons in top quark decays. No indication for charged Higgs boson production in the tauonic or leptophobic model is found. Upper limits at 95% CL on the $B(t \to H^+b)$ branching ratios are derived in different scenarios depending on the values of $B(H^+ \to c\bar{s})$ and $B(H^+ \to \tau^+\nu)$. For the leptophobic model, $B(t \to H^+b) > 0.22$ is excluded for the M_{H^+} range between 80 and 155 GeV. For the tauonic model, $B(t \to H^+b) > 0.15 - 0.19$ are excluded depending on M_{H^+}. In this model we have also performed a model-independent measurement and excluded $B(t \to H^+b) > 0.12 - 0.26$ depending on M_{H^+}.

We interpret the results in different models and exclude regions in $[\tan\beta, M_{H^+}]$ parameter space. For the m_h-max scenario, for example, M_{H^+} values up to 149 GeV are excluded. These are the most restrictive limits to date in direct searches for charged Higgs boson production in top quark decays.
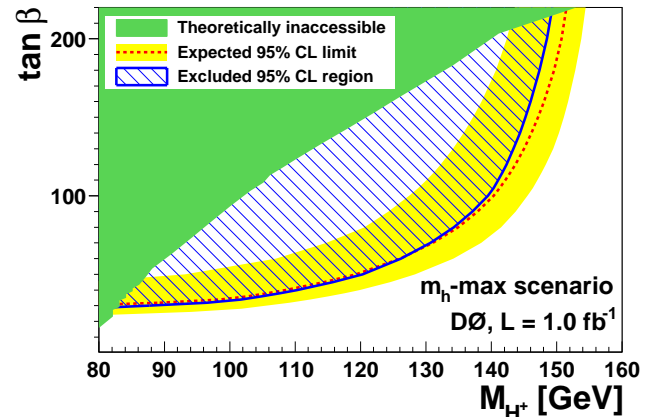
FIG. 8: Excluded region of $[\tan\beta, M_{H^+}]$ parameter space in the MSSM for the m_h-max scenario. The yellow band shows the ± 1 SD band around the expected limit (Color version online).

[a] Visitor from Augustana College, Sioux Falls, SD, USA.
[b] Visitor from Rutgers University, Piscataway, NJ, USA.
[c] Visitor from The University of Liverpool, Liverpool, UK.
[d] Visitor from Centro de Investigacion en Computacion - IPN, Mexico City, Mexico.
[e] Visitor from ECFM, Universidad Autonoma de Sinaloa, Culiacán, Mexico.
[f] Visitor from Universität Bern, Bern, Switzerland.
[g] Visitor from Universität Zürich, Zürich, Switzerland.

[1] D. J. H. Chung, L. L. Everett, G. L. Kane, S. F. King, J. Lykken and L-T. Wang, Phys. Rept. **407**, 1 (2005).
[2] Throughout the Letter, H^+ and W^+ also refer to the charge conjugate state.
[3] V. M. Abazov et al. [D0 Collaboration], Phys. Rev. D **80** (2009).
[4] Y. Grossman, Nucl. Phys. **B426**, 355 (1994).
[5] A. G. Akeroyd, arXiv:hep-ph/9509203 (1995).
[6] M. S. Carena, S. Mrenna and C. E. M. Wagner, Phys. Rev. D **62**, 055008 (2000).
[7] J. S. Lee, Y. Peters, A. Pilaftsis and C. Schwanenberger, arXiv:0909.1749 [hep-ph].
[8] M. S. Carena, S. Heinemeyer, C. E. M. Wagner and G. Weiglein, Eur. Phys. J. C **26**, 601 (2003).
[9] V. M. Abazov et al. [D0 Collaboration], Phys. Lett. B **679**, 177 (2009).
[10] M.L. Mangano et al., JHEP **07**, 001 (2003).
[11] T. Sjöstrand et al., Comput. Phys. Commun. **135**, 238 (2001).
[12] E.E. Boos et al., Phys. Atom. Nucl. **69**, 1317 (2006).
[13] R. Brun and F. Carminati, CERN Program Library Long Writeup W5013, 1993 (unpublished).
[14] S. Moch and P. Uwer, Phys. Rev. D **78**, 034003 (2008); S. Moch and P. Uwer, private communications.
[15] Tevatron Electroweak Working Group and CDF Collaboration and D0 Collaboration, arXiv:0903.2503 [hep-ex] (2009).
[16] G. Feldman and R. Cousins, Phys. Rev. D **57**, 3873 (1998).
[17] CDF Collaboration, A. Abulencia et al., Phys. Rev. Lett. **96**, 042003 (2006).
[18] V. M. Abazov et al. [D0 Collaboration], Phys. Rev. D **80**, 051107 (2009).
[19] OPAL Collaboration, G. Abbiendi et al., arXiv:0812.0267 [hep-ex]; ALEPH Collaboration, A. Heister et al., Phys. Lett. B **543**, 1 (2002); L3 Collaboration, P. Achard et al., Phys. Lett. B **575**, 208 (2003); DELPHI Collaboration, J. Abdallah et al., Eur. Phys. J. C **34**, 399 (2004); ALEPH, DELPHI, L3 and OPAL Collaborations, the LEP working group for Higgs boson searches, arXiv:hep-ex/0107031.
[20] ALEPH, DELPHI, L3 and OPAL Collaborations, S. Schael et al., Eur. Phys. J. C **47**, 547 (2006).
[21] Since this model cannot be realized in the MSSM without further modifications, higher order SUSY corrections are not included.

[22] M. Frank, T. Hahn, S. Heinemeyer, W. Hollik, H. Rzehak and G. Weiglein, JHEP **0702**, 047 (2007); G. Degrassi, S. Heinemeyer, W. Hollik, P. Slavich and G. Weiglein, Eur. Phys. J. C **28**, 133 (2003); S. Heinemeyer, W. Hollik and G. Weiglein, Eur. Phys. J. C **9**, 343 (1999); S. Heinemeyer, W. Hollik and G. Weiglein, Comput. Phys. Commun. **124**, 76 (2000).

[23] J. S. Lee, M. Carena, J. Ellis, A. Pilaftsis and C. E. M. Wagner, Comput. Phys. Commun. **180**, 312 (2009); M. S. Carena, J. R. Ellis, A. Pilaftsis and C. E. M. Wagner, Nucl. Phys. **B586**, 92 (2000); M. S. Carena, J. R. Ellis, A. Pilaftsis and C. E. M. Wagner, Nucl. Phys. **B625**, 345 (2002); M. S. Carena, J. R. Ellis, A. Pilaftsis and C. E. M. Wagner, Phys. Lett. **B495**, 155 (2000).